

Global trends in the interplane penetration depth of layered superconductors

S.V. Dordevic, E.J. Singley and D.N. Basov

Department of Physics, University of California, San Diego, La Jolla, CA 92093

Seiki Komiya and Yoichi Ando

Central Research Institute of Electric Power Industry, Tokyo, Japan

E. Bucher*

Lucent Technologies, Murray Hill, NJ 07974

C.C. Homes and M. Strongin

Department of Physics, Brookhaven National Laboratory, Upton, NY 11973

We report on generic trends in the behavior of the interlayer penetration depth λ_c of several different classes of quasi two-dimensional superconductors including high- T_c cuprates, Sr_2RuO_4 , transition metal dichalcogenides and organic materials of the $(BEDT - TTF)_2X$ - series. Analysis of these trends reveals two distinct patterns in the scaling between the values of λ_c and the magnitude of the c -axis DC conductivity σ_{DC} : one realized in the systems with a ground state formed out of well defined quasiparticles and the other seen in systems in which the quasiparticles are not well defined. The latter pattern is found primarily in under-doped cuprates and indicates a dramatic enhancement (factor $\simeq 10^2$) of the energy scale Ω_C associated with the formation of the condensate compared to the data for conventional materials. We discuss the implication of these results on the understanding of superconductivity in high- T_c cuprates.

I. INTRODUCTION

The formation of the superconducting condensate in elemental metals and their alloys is well understood within the theory of Bardeen, Cooper and Schrieffer (BCS) in terms of a pairing instability in the ensemble of Fermi liquid (FL) quasiparticles. Applicability of the FL description to high- T_c cuprate superconductors is challenged by remarkable anomalies found in both the spin- and charge response of these compounds in the normal state¹. Because quasiparticles are not well defined at $T > T_c$ in most cuprates it is natural to inquire into the distinguishing characteristics of the superconducting condensate which appears to be built from entirely different "raw material". Infrared spectroscopy is perfectly suited for this task. Indeed, the analysis of the optical constants in the far infrared (IR) unfolds the process of the formation of the condensate $\delta(0)$ -peak in the dynamical conductivity² and also gives insight into the single-particle excitations in the system both above and below T_c .

In this paper we focus on the inter-plane properties of high- T_c superconductors. We will show that the distinctions in the behavior of the condensate in conventional superconductors and high- T_c cuprates are most radical in the case of the c -axis inter-plane response. The analysis of the generic trends seen in the behavior of the c -axis condensate (correlation between the penetration depth λ_c and the DC conductivity σ_{DC}) allows us to infer the energy scale Ω_C associated with the development of the superfluid in the cuprates. This energy scale may dramatically exceed the energy gap in systems lacking well defined quasiparticles at $T > T_c$ (primarily in under-

doped cuprates³). We discuss a connection between the magnitude of Ω_C and the nature of the normal state response.

II. EXPERIMENTAL PROCEDURES

The response of the superconducting condensate can be investigated through the IR experiments probing the complex conductivity $\sigma(\omega) = \sigma_1(\omega) + i\sigma_2(\omega)$ of a superconductor. At $T < T_c$ the real part of the conductivity can be written as:

$$\sigma_1^{SC}(\omega) = \frac{\rho_s}{8}\delta(0) + \sigma_1^{reg}(\omega). \quad (1)$$

The delta-peak term represents the response of the condensate with the superfluid density $\rho_s = 4\pi n_s e^2/m^*$ proportional to the concentration of superconducting carriers n_s and inversely proportional to their effective mass m^* . The second term on the right-hand side of the Eq. 1 is usually referred to as the regular component and represents the conductivity that is NOT due to the superconducting carriers. It may include conductivity due to unpaired carriers at $T < T_c$ at finite frequencies, phonons, interband transitions, magnons, etc. Commonly, the condensate stiffness is characterized through the penetration depth $\lambda = c/\sqrt{\rho_s}$, the notation we will use in this paper.

In order to discuss several techniques that can be exploited to determine the interlayer penetration depth of an anisotropic superconductor we turn to our data for $\text{La}_{1.83}\text{Sr}_{0.17}\text{CuO}_4$ (La214) with $T_c \simeq 36$ K (Fig. 1). Large single crystals were grown using traveling-solvent floating-zone technique⁴ and were carefully annealed to remove excess oxygen. The crystallographic axes were

determined by Laue diffraction and the samples were then cut into platelets with the ac planes parallel to the wide face. The error in the axes directions is less than 1° . Near-normal-incidence reflectance measurements were performed at UCSD in the frequency range between $10\text{-}48,000\text{ cm}^{-1}$ ($1\text{ meV} - 6\text{ eV}$). The complex conductivity $\sigma(\omega)$ and complex dielectric function $\epsilon(\omega) = \epsilon_1(\omega) + i\epsilon_2(\omega)$ were inferred from $R(\omega)$ using Kramers-Kronig (KK) analysis. The low and high frequency extrapolations have negligible effect on the data in the measured frequency interval.

Below we outline common analysis techniques used to determine the penetration depth from the results of IR studies.

1) Raw c -axis reflectance of most high- T_c superconductors at $T \ll T_c$ exhibits a sharp plasma edge. In the case of $\text{La}_{1.83}\text{Sr}_{0.17}\text{CuO}_4$ this feature is located at $\sim 85\text{ cm}^{-1}$ (Fig. 1, panel A). This behavior is in contrast to the featureless normal state reflectance. The position of the plasma edge is determined by the screened plasma frequency $\tilde{\omega}_p$, from which the penetration depth can be obtained as $c^2/\lambda^2 = \tilde{\omega}_p^2 \epsilon_\infty$ (Ref. 5). In the latter equation ϵ_∞ is the real part of the dielectric constant $\epsilon_1(\omega)$ at frequencies above the plasma edge. The numerical value of ϵ_∞ is somewhat ambiguous and introduces error in the result for λ_c . This technique has been employed in Ref. 6–9.

2) In a BCS superconductor the formation of the condensate is adequately described with the Ferrel-Glover-Tinkham (FGT) sum rule:

$$\rho_s = \frac{c^2}{\lambda^2} = \int_{0+}^{\Omega_C} [\sigma_1^N(\omega) - \sigma_1^{reg}(\omega)] d\omega \quad (2)$$

where $\sigma_1^N(\omega)$ is the normal state conductivity at T_c and the upper integration limit Ω_C is of the order of the gap energy. The upper cut-off issue for cuprates will be discussed in detail below. According to this sum rule the area "missing" from the normal state conductivity (shaded region in Fig. 1 B) is recovered under the $\delta(0)$ -peak. This technique may somewhat underestimate the magnitude of λ_c because, at least in underdoped cuprates the superfluid density is accumulated from a broad energy region significantly exceeding the gap energy^{2,8,10,11}. This method has been used for the analysis of the penetration depth in Ref. 12–14.

3) Finally, the most commonly used method of extracting λ_c is based on the examination of the imaginary part of the complex optical conductivity. By KK transformation, the δ -peak at $\omega = 0$ in the real part of the optical conductivity implies that the imaginary part has the form $\sigma_2(\omega) = c^2/(4\pi\omega\lambda^2)$. Therefore the magnitude of λ_c can be estimated from $\omega \times \sigma_2(\omega)$ in the limit of $\omega \rightarrow 0$. (the gray line in panel C of Fig. 1 or the dotted line in panel D) (Ref. 2,6,8,10,11,15–18).

While method 3 is very well suited to quantify the magnitude of the penetration depth, this technique also may introduce systematic errors. Strictly speaking the

relation $\sigma_2(\omega) = c^2/(4\pi\omega\lambda^2)$ is valid only if $\sigma_1^{reg}(\omega) = 0$. Typically, this is not the case in high- T_c superconductors which all show residual absorption in the far-IR conductivity. This absorption may be (in part) connected with d -wave symmetry of the order parameter in cuprates¹ leading to gapless behavior at any finite temperature. Data displayed in Fig. 1 B clearly shows non-vanishing IR conductivity down to the lowest T and ω . A finite regular contribution to $\sigma_1(\omega)$ implies a finite contribution to $\sigma_2(\omega)$. Owing to this contribution the spectra of $\sigma_2(\omega)$ acquire a complicated frequency dependence that may significantly differ from the $1/\omega$ form (Fig. 1 C, D). Moreover, the magnitude of the penetration depth extracted from such a spectrum is likely to be underestimated, even if the product $\sigma_2(\omega) \times \omega$ is taken at the lowest experimentally accessible frequencies.

Systematic errors in the magnitude of λ connected with $\sigma_1^{reg}(\omega) > 0$ can be eliminated using the following procedure. The intrinsic value of the penetration depth can still be determined from $\sigma_2(\omega)$, if the imaginary part of the conductivity is corrected by $\sigma_2^{reg}(\omega)$ characterizing all screening effects that are not due to superconducting carriers at $T < T_c$:

$$\sigma_2(\omega) - \sigma_2^{reg}(\omega) = \frac{c^2}{4\pi\omega\lambda^2}. \quad (3)$$

To determine $\sigma_2^{reg}(\omega)$ we employ a KK-like transformation:

$$\sigma_2^{reg}(\omega) = -\frac{2\omega}{\pi} \int_{0+}^{\infty} \frac{\sigma_1^{reg}(\omega')}{\omega'^2 - \omega^2} d\omega'. \quad (4)$$

The result of the application of the correction procedure for the imaginary part of the conductivity is presented in Fig. 1 D. It appears that after subtraction of $\sigma_2^{reg}(\omega)$ the remaining contribution to the conductivity reveals a $1/\omega$ behavior over an extended frequency region, supporting the soundness of the procedure proposed here. We emphasize again that *no other* correction procedure besides that described by Eqs. 3 and 4 has been used. In the case of $\text{La}_{1.83}\text{Sr}_{0.17}\text{CuO}_4$ the latter procedure has lead only to minor correction of the absolute value of λ_c ($\sim 18\%$). That is because the absolute value of $\sigma_1^{reg}(\omega)$ is relatively small and is constant throughout far-IR (Fig. 1 B). However, such a correction can be much more significant for the overdoped samples which often show stronger Drude-like contribution in $\sigma_1^{reg}(\omega)$ spectra. Panel D also shows a frequently used approximation to the method we have just outlined: instead of subtracting $\sigma_2^{reg}(\omega)$, one subtracts $\sigma_2(\omega, T_c)$ from $\sigma_2(\omega, T \ll T_c)$. The resulting curve looks somewhat better than the uncorrected one, but still yields an enhanced value of $\omega \times \sigma_2(\omega)$ in the limit of $\omega \rightarrow 0$.

III. UNIVERSAL C-AXIS PLOT

The c -axis penetration depth in a layered superconductor can be determined from IR experiments^{2,6–18} as

described in the previous section. In addition, several other experimental techniques including magnetization measurements^{19–26}, microwave absorption^{27–33}, and vortex imaging^{34,35} can be used to determine the magnitude of λ_c . Regardless of the method employed, the inter-layer penetration depth in several families of cuprates reveals a universal scaling behavior with the magnitude of $\sigma_{DC}(T = T_c)$ (Fig. 2)¹⁵: the absolute value of λ_c is systematically suppressed with the increase of the normal state conductivity³⁶. The scaling is obeyed primarily in under-doped cuprates (blue symbols in Fig. 2). The deviations from the scaling are also systematic and are most prominent in over-doped phases (red symbols in Fig. 2). Such deviations are a direct consequence of a well-established fact: on the over-doped side of the phase diagram σ_{DC} increases whereas λ_c is either unchanged or may show a minor increase^{10,16,37}.

We find a similar scaling pattern between λ_c and σ_{DC} in other classes of layered superconductors, including organic materials, transition metal dichalcogenides and Sr_2RuO_4 (Fig. 2). While the non-cuprate data set is not nearly as dense, the key trend is analogous to the one found for cuprates. The slope of the $\lambda_c - \sigma_{DC}$ dependence is also close for both cuprates and non-cuprate materials. The principal difference is that the cuprates universal line is shifted down by approximately one order of magnitude in λ_c . The latter result shows that the superfluid density ($\propto 1/\lambda^2$) is significantly enhanced in under-doped cuprates compared to non-cuprate materials with the same DC conductivity.

Possible origins of the $\lambda_c - \sigma_{DC}$ correlation were recently discussed in the literature³⁸. A plausible qualitative account of this effect can be based on the FGT sum rule, Eq. 2. For a dirty limit superconductor $\sigma_1^N(\omega) \approx \sigma_{DC}$, and Eq. 2 can be approximated as:

$$\rho_s = \frac{c^2}{\lambda^2} \approx 2\Delta\sigma_{DC}. \quad (5)$$

Such an approximation is possible because within the BCS model the energy scale Ω_C from which the condensate is collected is of the order of magnitude of the gap: $\Omega_C \simeq 2\Delta \simeq 3 - 5kT_c$. A connection between $1/\lambda^2$, σ_{DC} , and 2Δ is illustrated in the inset of Fig. 2. In the dirty limit the magnitude of σ_{DC} sets the amount of spectral weight available in the normal state conductivity whereas the magnitude of $\Omega_C \simeq 2\Delta$ defines the fraction of this weight which is transferred into condensate at $T < T_c$. Therefore, the magnitude of λ_c can be expected to systematically decrease with the enhancement of the DC conductivity, in accord with the FGT sum rule. Notably, an approximate form (Eq. 5) yields the $\lambda_c - \sigma_{DC}$ scaling with the power law $\alpha = 1/2$ which is close to $\alpha = 0.59$ seen in Fig. 2.

The strong condensate density in the cuprates can be understood in terms of the dramatic enhancement of the energy scale Ω_C over the magnitude of the energy gap. This can be seen through a comparison of the universal

scaling patterns observed for cuprates and of a similar pattern detected for non-cuprate superconductors. The energy scale associated with the condensate formation for materials on the upper line, which for most conventional materials in Fig. 2 is close to estimates of the gap, is of the order of 1-3 meV. In Sr_2RuO_4 for example $2\Delta = 2.2$ meV based on Andreev reflection measurements.³⁹ If Eq. 5, in the form $\rho_s = c^2/\lambda^2 \approx \Omega_C\sigma_{DC}$ appropriate for cuprates, is employed to describe the difference between the upper and the lower lines in Fig. 2, then one can conclude that the corresponding scale for underdoped cuprates is ~ 100 times greater, i.e. of the order 0.1 - 0.3 eV. This assessment of Ω_C is supported by the explicit sum rule analysis for several cuprates^{2,11} and also makes Ω_C the largest energy scale in the problem of cuprate superconductivity⁴⁰.

Data points in Fig. 2 for overdoped materials support the notion that the $\lambda_c - \sigma_{DC}$ plot provides means to learn about the energy scale associated with the condensate formation. Deflection of the over-doped cuprates from the universal line implies that Ω_C is gradually suppressed with the increased carrier density. This trend is common for $\text{Tl}_2\text{Ba}_2\text{CuO}_{6+\delta}$ (Tl2201), La214 and $\text{YBa}_2\text{Cu}_3\text{O}_{7-\delta}$ (YBCO) materials (see Fig. 2). Integration of the conductivity for all these overdoped materials shows that the FGT sum rule is exhausted at energies as low as 0.08 eV (Ref. 10,11).

In BCS superconductors Ω_C is related to 2Δ , and therefore to T_c . In cuprates we find no obvious connection between the broad energy scale Ω_C and the critical temperature T_c . While scaling of λ_c by the magnitude of T_c does reduce the "scattering" of the data points^{33,38}, the two distinct $\lambda_c - \sigma_{DC}$ patterns persist even if such scaling is implemented. Similarly, the difference between the two lines in Fig. 2 cannot be accounted for by differences in T_c . In particular, the critical temperature of strongly under-doped La214 materials is nearly the same as that of the several ET-compounds ($\simeq 12 - 15$ K). Nevertheless, the penetration depth is dramatically enhanced in the latter systems.

IV. IN-PLANE QUASIPARTICLES AND INTER-PLANE TRANSPORT

A quick inspection of the materials in Fig. 2 suggests that the $\simeq 3$ meV scale (top line) is observed in systems in which superconductivity emerges out of a normal state with well defined quasiparticles, whereas the enhanced value of $\Omega_C \simeq 0.3$ eV is found in underdoped cuprates for which the quasiparticle concept may not apply (bottom line). The experiments which in our opinion are most relevant to this classification include quantum oscillations of the low- T inter-layer resistivity (and of other quantities) in high magnetic fields⁴¹. Quantum oscillations can be viewed as a direct testimony of long-lived quasiparticles capable of propagating coherently between the layers. Indeed, quantum oscillations have been observed in

2D organic superconductors^{41,42}, 2H-NbSe₂ (Ref. 43) and Sr₂RuO₄ (Ref. 44). On the contrary, quantum oscillations have never been reported for under-doped cuprates. The lack of coherence in the *c*-axis transport in these materials indicates that the ground state of cuprates may be fundamentally different.

Signatures of coherent and incoherent behavior can also be recognized in the spectra of the *c*-axis conductivity. A hallmark of a coherent response is the Drude peak seen in $\sigma_1(\omega)$ of metals. Notably, a similar feature has never been found in underdoped compounds (forming the lower line in Fig. 2). The electronic contribution to $\sigma_1(\omega)$ in these materials is usually structureless which is commonly associated with the incoherent (diffusive) motion of charge carriers across the planes. On the contrary, many materials that belong to the upper line in Fig. 2 demonstrate a familiar Drude-like behavior. This kind of behavior has been found in Sr₂RuO₄ (Ref. 45) and is also shown in our data⁴⁶ for inter-plane response of 2H-NbSe₂ (Fig. 3, top-right panel). In both cases, the width of the peak decreases at low temperatures, which is characteristic of the response of ordinary metals⁴⁷. As for the over-doped cuprates (located in a cross-over region between the two lines in Fig. 2) their conductivity is indicative of the formation of the Drude-like peak (see for example $\sigma_c(\omega)$ for YBa₂Cu₃O₇; Fig. 3, top-middle panel), which is becoming more pronounced with increased carrier density⁴⁸.

Analysis of the anisotropic carrier dynamics in several layered superconductors indicates that the degree of coherence in the interplane transport may be related to the strength of inelastic scattering within the conducting planes. The bottom panels in Fig. 3 show the *in-plane* scattering rate (inverse lifetime) $1/\tau_{ab}(\omega)$ (Ref. 49) for the layered compounds corresponding to the top three panels⁵⁰. In all these systems $1/\tau_{ab}(\omega) \propto \omega$ over an extended frequency interval (up to 3,000 cm⁻¹)⁵¹. An important feature of the data displayed in Fig. 3 is that as doping is increased from underdoped YBa₂Cu₃O_{6.6} to optimally doped YBa₂Cu₃O_{6.95} the absolute values of $1/\tau_{ab}(\omega)$ decrease. A similar trend is observed in other cuprate families⁵²⁻⁵⁵. The shaded regions in Fig. 3 represent Landau Fermi liquid (LFL) regime, where the quasiparticles are well defined, i.e. the magnitude of the scattering rate is smaller than energy ($1/\tau(\omega) \leq \omega$). In 2H-NbSe₂ $1/\tau_{ab}(\omega, 10K)$ is in the LFL regime over the entire frequency interval displayed in Fig. 3. However this is not the case for the two cuprates discussed. We believe that these differences in absolute values may have a profound effect on the *interplane* transport. In 2H-NbSe₂ where the in-plane quasiparticles are well defined the interplane transport is also coherent, and is characterized by a narrow Drude-like mode whose width decreases with temperature (Fig. 3, top-right panel). On the other hand, in YBa₂Cu₃O_{6.6}, which is lacking well defined quasiparticles, the interplane transport is incoherent, with $\sigma_1(\omega)$ being dominated by optical phonons (Fig. 3, top-right). As for the over-doped YBa₂Cu₃O₇ (Fig. 3, bottom-

middle) the optical conductivity of this compound is in between these two opposite limits. Figure 3 therefore supports the notion that long-lived *in-plane* quasiparticles may be one of the necessary prerequisites for coherent *out-of-plane* transport.

V. GLOBAL TRENDS IN LAYERED SUPERCONDUCTORS

To summarize the experimental results reported in this work, we wish to stress the following points: *i*) two distinct patterns in $\lambda_c - \sigma_{DC}$ correlation (Fig. 2) are indicative of a dramatic difference ($\simeq 10^2$) in the energy scale Ω_C from which the interlayer condensate is collected; *ii*) the pattern with the typical energy scale of $\Omega_C \simeq 3$ meV is realized in the materials with the coherent transport between the planes, whereas the one with $\Omega_C \simeq 300$ meV is found in underdoped cuprate superconductors with an incoherent response; *iii*) over-doped cuprates reveal a cross-over between the two behaviors; *iv*) coherence in the interlayer transport correlates with the strength of inelastic scattering within the conducting planes (Fig. 3).

These results allow us to draw several conclusions regarding features of the superconducting condensate in different layered systems:

- The symmetry of the order parameter seems to be unrelated to trends seen in the *c*-axis condensate response. Indeed, the upper line in Fig. 2 is formed by *s*-wave transition metal dichalcogenides, *p*-wave Sr₂RuO₄ and organic materials for which both *s*- and *d*-wave states have been proposed⁴¹, while *d*-wave high- T_c materials form the lower line and the crossover region between the lines.
- Electrodynamics of the systems on the top line at $T \ll T_c$ is determined by the magnitude of the gap (and hence by T_c), in general agreement with the BCS theory. It is therefore hardly surprising that the trend initiated by 2D superconductors is also followed in 1-dimensional organic conductors, as well as by more conventional systems such as Nb Josephson junctions, bulk Nb and Pb or amorphous $\alpha\text{Mo}_{1-x}\text{Ge}_x$ (see Fig. 2).
- While the pseudogap state has been shown to be responsible for the anomalous superfluid response of the underdoped cuprates^{2,11}, the characteristic pseudogap temperature $T^* = 90 - 350$ K is still much lower than our estimate of Ω_C for these materials (0.1 - 0.3 eV, i.e. 1,000 - 3,000 K).
- Unlike BCS superconductors where T_c is determined by 2Δ and therefore by Ω_C , the critical temperature T_c in cuprates correlates with neither 2Δ nor Ω_C .

In conclusion, analyzing a large amount of experimental data, we found two distinctly different patterns in $\lambda_c - \sigma_{DC}$ scaling in layered superconductors. Based on the universal *c*-axis plot, we inferred a broad energy scale Ω_c relevant for pair formation in underdoped cuprates. This result is consistent with the idea that the superconducting transition in the cuprates is driven by a lowering

of the electronic kinetic energy⁷². We argue that the appearance of such an energy scale is fundamentally related to the incoherent c-axis transport, which on the other hand may be related to poorly defined in-plane quasiparticles. A quantitative account of the distinct energy scales associated with the condensate is a challenge for models attempting to solve the puzzle of cuprate superconductivity.

The research at UCSD is supported by NSF, DoE and the Research Corporation. The work at Brookhaven National Laboratory is supported, in part, by the U.S. Department of Energy, Division of Materials Science, under Contract No. DE-AC02-98CH10886.

* Also at Fakultät für Physik, Universität Konstanz, D-78457 Konstanz, Germany.

Electronic address: sasa@physics.ucsd.edu

-
- ¹ J. Orenstein and A.J. Millis, *Science* **288**, 468 (2000).
- ² D.N. Basov, S.I. Woods, A.S. Katz, E.J. Singley, R.C. Dynes, M. Xu, D.G. Hinks, C.C. Homes and M. Strongin, *Science* **283**, 49 (1999).
- ³ Under-doped cuprates are compounds whose carrier doping level is smaller than optimal, i.e. the one that gives the highest T_c .
- ⁴ Y. Ando, A.N. Lavrov, S. Komiya, K. Segawa and X.F. Sun, *Phys.Rev.Lett.* **87**, 017001 (2001).
- ⁵ T. Timusk and D.B. Tunnner, in *Physical properties of high temperature superconductors I*, edited by D.M. Ginsberg, World Scientific (1989).
- ⁶ S. Uchida and K. Tamasaku, *Phys.C* **293**, 1 (1997).
- ⁷ T. Motohashi, J. Shimoyama, K. Kitazawa, K. Kishio, K.M. Kojima, S. Uchida and S. Tajima, *Phys.Rev.B* **61**, 9269 (2000).
- ⁸ E.J. Singley, D.N. Basov, K. Kurahashi, T. Uefuji and K. Yamada, *Phys.Rev.B* **64**, 224503 (2001).
- ⁹ A.A. Tsvetkov, D. van der Marel, K.A. Moler, J.R. Kirtley, J.L. de Boer, A. Meetsma, Z.F. Ren, N. Kolesnikov, D. Dulic, A. Damascelli, M. Gruninger, J. Schutzmann, J.W. van der Eb, H.S. Somal, J.H. Wang, *Nature*, **395**, 360 (1998).
- ¹⁰ A.S. Katz, S.I. Woods, E.J. Singley, T.W. Li, M. Xu, D.G. Hinks, R.C. Dynes and D.N. Basov, *Phys.Rev.B* **61**, 5930 (2000).
- ¹¹ D.N. Basov, C.C. Homes, E.J. Singley, M. Strongin, T. Timusk, G. Blumberg and D. van der Marel, *Phys.Rev.B* **63**, 134514 (2001);
- ¹² C. Bernhard, D. Munzar, A. Wittlin, W. Konig, A. Golnik, C.T. Lin, M. Klayer, T. Wolf, G. Muller-Vogt and M. Cardona, *Phys.Rev.B* **59**, 6631 (1999)
- ¹³ J. Schutzmann, S. Tajima, S. Miyamoto and S. Tanaka, *Phys.Rev.Lett.* **73**, 174 (1994).
- ¹⁴ S. Tajima, J. Schutzmann, S. Miyamoto, I. Terasaki, Y. Sato and R. Hauff, *Phys.Rev.B* **55**, 6051 (1997).
- ¹⁵ D.N. Basov, T. Timusk, B. Dabrowski and J.D. Jorgensen, *Phys.Rev.B* **50**, 3511 (1994).
- ¹⁶ S. Uchida, K. Tamasaku and S. Tajima, *Phys.Rev.B* **53**, 14558 (1996).
- ¹⁷ C.C.Homes, T. Timusk, D.A. Bonn, R. Liang and W.N. Hardy, *Phys.C* **254**, 265 (1995).
- ¹⁸ D.N. Basov, H.A. Mook, B. Dabrowski and T. Timusk, *Phys.Rev.B* **52**, 13141 (1995).
- ¹⁹ P. de Trey, S. Gygax and J.-P. Jan, *J.Low Temp.Phys.* **11**, 421 (1973).
- ²⁰ D.J. Huntley and R.F. Frindt, in *Physics and chemistry of materials with layered structures*, Reidel Publishing Company, 1976.
- ²¹ K. Onabe, M. Naito and S. Tanaka, *J.Phys.Soc.Jap.* **45** 50 (1978).
- ²² A. Carrington, I.J. Bonalde, R. Prozorov, R.W. Giannetta, A.M. Kini, J. Schlueter, H.H. Wang, U. Geiser and J.M. Williams, *Phys.Rev.Let.* **83**, 4172 (1999).
- ²³ J.R. Cooper, L. Forro and B. Keszei, *Nature* **343**, 444 (1990).
- ²⁴ H. Taniguchi, H. Sato, Y. Nakazawa and K. Kanoda, *Phys.Rev. B* **53**, 8879 (1996).
- ²⁵ S. Wanka, D. Beckmann, J. Wosnitza, E. Balthes, D. Schweitzer, W. Strunz and H.J. Keller, *Phys.Rev. B* **53**, 9301 (1996).
- ²⁶ K. Yoshida, Y. Maeno, S. Nishizaki and T. Fujita, *Phys.C* **263**, 519 (1996).
- ²⁷ A. Pimenov, A.V. Pronin, A. Loidl, U. Michelucci, A.P. Kampf, S.I. Krasnovobodtsev, V.S. Nozdrin, D. Rainer, *Phys.Rev.B* **62**, 9822 (2000).
- ²⁸ T. Shibauchi, M. Sato, A. Mashio, T. Tamegai, H. Mori, S. Tajima and S. Tanaka, *Phys.Rev. B* **55**, 11977 (1997).
- ²⁹ M. Dressel, O. Klein, G. Gruner, K.D. Carlson, H.H. Wang and J.M. Williams, *Phys.Rev. B* **50**, 13603 (1994).
- ³⁰ R. Prozorov, R.W. Giannetta, J. Schlueter, A.M. Kini, J. Mohtasham, R.W. Winter and G.L. Gard, *Phys.Rev.B* **63**, 052506 (2001).
- ³¹ A.V. Pronin, M. Dressel, A. Pimenov, A. Loidl, I.V. Roshchin and L.H. Greene, *Phys.Rev.B* **57**, 14416 (1998).
- ³² O. Klein, E.J. Nicol, K. Holczer and G. Gruner, *Phys.Rev.B* **50**, 6307 (1994).
- ³³ T. Shibauchi, H. Kitano, K. Uchinokura, A. Maeda, T. Kimura and K. Kishio, *Phys.Rev.Lett.* **72**, 2263 (1994).
- ³⁴ J.R. Kirtley, K.A. Moler, G. Villard and A. Maignan, *Phys.Rev.Lett.* **81**, 2140 (1998).
- ³⁵ K.A. Moler, J.R. Kirtley, D.G. Hinks, T.W. Li and M. Xu, *Science* **279**, 1193 (1998);
- ³⁶ Whenever available λ_c and σ_{DC} values obtained from IR spectroscopy were used, and as shown here the errors of such measurements do not exceed 15-20 %. This error includes the error introduced by the uncertainty of reflectance measurements, which is typically around 1 %. When IR spectroscopic data were not available (particularly for the compounds on the top line in Fig. 2), we used the results from other experimental techniques mentioned in the text. Typical errors, as reported in the original publications, are: <10 % for microwave absorption³¹, ~20 % for magnetization²², <30 % for vortex imaging³⁵ and ~ 5 % for resistivity (i.e. $1/\sigma_{DC}$) measurements. When the results from different measurements on the same com-

pound differed substantially, for example λ_c values for $\kappa(BEDT - TTF)_2Cu[N(CS)_2]Br$ (Ref. 22,29), they were both shown in Fig. 2. We emphasize that errors as high as 20 % cannot in any significant way change a plot that spans over several orders of magnitude.

³⁷ C. Panagopoulos, J.R. Cooper, T. Xiang, Y.S. Wang and C.W. Chu, Phys.Rev.B, **61**, 3808 (2000).

³⁸ W.Kim and J.P. Carbotte, Phys.Rev. B **61**, 11886 (2000); Y.Ohashi, J.Phys.Soc.Jpn **69**, 659 (2000); P.J. Hirschfeld, S.M. Quinlan and D.J. Scalapino, Phys.Rev. B **55**, 12742 (1997); S. Chakravarty, Hae-Young Kee and E. Abrahams, Phys.Rev.Lett. **82**, 2366, (1999).

³⁹ F. Laube, G. Goll, H.v. Lohneysen, M. Fogelstrom, and F. Lichtenberg, Phys.Rev.Lett. **84**, 1595 (2000).

⁴⁰ The sum rule arguments discussed in this section may help one understand the rationale behind the universal $\lambda_c - \sigma_{DC}$ scaling in underdoped cuprates. That is despite the fact that the superconducting energy gap is not well-defined in the interlayer conductivity of these materials. The gap-less response of cuprates is exemplified in the top-left panel of Fig. 3 displaying $\sigma_1(\omega)$ data for $YBa_2Cu_3O_{6.6}$ with $T_c \simeq 60$ K. The normal state conductivity is suppressed as the sample is cooled down to T_c , with a transfer of spectral weight to higher energies. Below T_c , one does not find any radical changes in the $\sigma_1(\omega)$ spectra. Most importantly, this system, along with all other under-doped compounds, shows significant absorption in the superconducting state so that $\sigma_1^{reg} > 0$. Therefore, in cuprates only a *small fraction* of the far-infrared spectral weight is contributing to the condensate. The latter result is in apparent conflict with the assumption $\sigma_1^{reg}(\omega < 2\Delta) \simeq 0$, which allows one to reduce Eq. 2 to an approximate form given by Eq. 5. However, the strong condensate density seen in the cuprates located on the universal line can be understood in terms of the dramatic enhancement of the energy scale Ω_C over the magnitude of the energy gap. This latter conclusion also follows from the explicit sum rule analysis for samples of underdoped $La_{2-x}Sr_xCuO_4$ (La214), $YBa_2Cu_3O_{7-\delta}$ (YBCO) and $Tl_2Ba_2CuO_{6+\delta}$ (Tl2201) materials, suggesting that Ω_C in these compounds exceeds 0.1-0.2 eV (Ref. 2,10,11).

⁴¹ J. Wosnitzer, *Fermi surfaces of low-dimensional organic metals and superconductors*, Berlin, New York; Springer (1996).

⁴² J. Singleton, P.A. Goddard, A. Ardavan, N. Harrison, S.J. Blundell, J.A. Schlueter and A.M. Kini, Phys.Rev.Lett. **87**, 117001 (2001).

⁴³ R. Corcoran, P. Meeson, Y. Onuki, P.-A. Probst, M. Springford, K. Takita, H. Harima, G.Y. Guo, B.L. Gyorffy, J.Phys.Cond.Mat. **6**, 4479 (1994).

⁴⁴ C. Bergemann, S.R. Julian, A.P. Mackenzie, S. NishiZaki and Y. Maeno, Phys.Rev.Lett. **84**, 2662 (2000).

⁴⁵ T. Katsufuji, M. Kasai, Y. Tokura, Phys.Rev.Lett. **76**, 126 (1996).

⁴⁶ S.V. Dordevic, D.N. Basov, R.C. Dynes and E. Bucher, Phys.Rev.B **64**, 161103 (2001).

⁴⁷ Earlier measurements of the *c*-axis infrared absorption proved applicability of conventional BCS electrodynamics to the 2H-NbSe₂ data. See: R.J. Kennedy and B.P. Clayman, Can.J.Phys. **62**, 776 (1984).

⁴⁸ We emphasize that the observation of a Drude-like mode

in the optical spectra is consistent with, but is not a definite proof of coherent interlayer transport. Similarly, the absence of a zero-energy mode, does not necessarily imply incoherent transport. Recent *c*-axis IR experiments on 2D organic superconductors⁵⁶ seem to indicate the absence of a Drude-like mode in these compounds. However, high magnetic field measurements^{41,42} undoubtedly show the existence of 3D Fermi surface, i.e. well defined quasiparticles that can propagate coherently between the layers.

⁴⁹ The scattering rate can be calculated from IR data as:

$$\frac{1}{\tau_{ab}(\omega)} = \frac{\omega_p^2}{4\pi} \frac{\sigma_1(\omega)}{\sigma_1^2(\omega) + \sigma_2^2(\omega)}, \quad (6)$$

where ω_p is the plasma frequency and can be obtained from the integration of the optical conductivity $\sigma_1(\omega)$ up to the frequency corresponding to the onset of interband absorption. See Ref. 55 for a review.

⁵⁰ Because the in-plane measurements of $YBa_2Cu_3O_7$ are not available, we have used $1/\tau_{ab}(\omega)$ data for $YBa_2Cu_3O_{6.95}$. We believe that this does not affect the conclusions of the paper in any significant way.

⁵¹ Many other 2D conductors also show a linear frequency dependence of the *in-plane* scattering rate. In particular this behavior has been reported for graphite⁵⁷, 2H-TaSe₂ and other transition metal dichalcogenides⁵⁸, and a variety of cuprates⁵²⁻⁵⁵.

⁵² D.N. Basov, R. Liang, B. Dabrowski, D.A. Bonn, W.N. Hardy and T. Timusk, Phys.Rev.Lett. **77**, 4090 (1996).

⁵³ A.V. Puchkov, P. Fournier, D.N. Basov, T. Timusk, A. Kapitulnik and N.N. Kolesnikov, Phys.Rev.Lett. **77**, 3212 (1996).

⁵⁴ L.D. Rotter, Z. Schlesinger, R.T. Collins, F. Holtzberg, C. Field, U.W. Welp, G.W. Crabtree, J.Z. Liu, Y. Fang, K.G. Vandervoort and S. Fleshler, Phys.Rev.Lett. **67**, 2741 (1991).

⁵⁵ A.V. Puchkov, D.N. Basov and T. Timusk, J.Phys.Cond.Mat. **8**, 10049 (1996).

⁵⁶ J.J. McGuire, T. Room, A. Pronin, T. Timusk, J.A. Schlueter, M.E. Kelly and A.M. Kini, Phys.Rev.B **64**, 94503 (2001).

⁵⁷ S. Xu, J. Cao, C.C. Miller, D.A. Mantell, R.J.D. Miller and Y. Gao, Phys.Rev.Lett. **76**, 483 (1996).

⁵⁸ T. Valla, A.V. Fedorov, P.D. Johnson, J. Xue, K.E. Smith and F.J. DiSalvo, Phys.Rev.Lett. **85**, 4759 (2000); V. Vescoli, L. Degiorgi, H. Berger and L. Forro, Phys.Rev.Lett. **81**, 453 (1998).

⁵⁹ E.J. Singley *et al.* unpublished.

⁶⁰ P. Garoche, J.J. Veyssie, P. Manuel and P. Molinie, Sol.Stat.Comm. **19**, 455 (1976).

⁶¹ J.J. Finley and B.S. Deaver, Sol.Stat.Comm. **36**, 493 (1980).

⁶² A.H. Thompson, F.R. Gamble and R.F. Koehler, Phys.Rev. B **5**, 2811 (1972).

⁶³ X. Su, F. Zuo, J.A. Schlueter, A.M. Kini and Jack M. Williams, Phys.Rev. B **58**, 2944 (1998). (resistivity)

⁶⁴ K. Kajita, Y. Nishio, S. Moriyama, W. Sasaki, R. Kato, H. Kobayashi and A. Kobayashi, Sol.Stat.Comm. **64**, 1279 (1987).

- ⁶⁵ X. Su, F. Zuo, J.A. Schlueter, J.M. Williams, P.G. Nixon, R.W. Winter and G.L. Gard, *Phys.Rev.B* **59**, 4376 (1999).
- ⁶⁶ H. Schwenk, K. Andres, F. Wudl and E. Aharon-Shalom, *Sol.State Commun.* **45**, 767 (1983).
- ⁶⁷ K. Murata, H. Anzai, G. Saito, K. Kajimura and T. Ishiguro, *J.Phys.Soc.Jpn.* **50**, 3529 (1981).
- ⁶⁸ Y. Maeno, H. Hashimoto, K. Yoshida, S. Nishizaki, T. Fujita, J.G. Bednorz and F. Lichtenberg, *Nature* **372**, 532 (1994).
- ⁶⁹ E. Goldobin, M.Yu. Kupriyanov, I.P. Nevirkovets, A.V. Ustinov, M.G. Blamire and J.E. Evetts, *Phys.Rev.B* **58**, 15078 (1998).
- ⁷⁰ S.J. Turneaure, T.R. Lemberger and J.M. Graybeal, *Phys.Rev.Lett.* **84**, 987 (2000).
- ⁷¹ C.C. Homes, T. Timusk, R. Liang, D.A. Bonn and W.N. Hardy, *Phys.Rev.Lett* **71**, 1645 (1993).
- ⁷² J.E.Hirsch, *Physica C* **199**, 305 (1992) and *Phys.Rev.B* **62**, 14498 (2000); M.R. Norman, M. Randeria, B. Janko and J.C. Campuzano, *Phys.Rev.B* **61**, 14742 (2000); L.B.Ioffe and A.J. Millis, *Phys.Rev.B* **61**, 9077 (2000); S. Chakravarty, *Eur.Phys.J.B* **5**, 337 (1998).

FIG. 1. Interlayer response of LSCO single crystals with $T_c=36$ K: reflectance $R(\omega)$ (panel A); real and imaginary parts of the conductivity (panels B and C) and the product $\sigma_2(\omega) \times \omega$ (panel D). The c -axis penetration depth can be determined from the IR data using several different techniques: from the position of the plasma minimum in $R(\omega)$, from integrating the difference between the $\sigma_1(\omega, T_c)$ and $\sigma_1(\omega, 10K)$ (Eq. 2); and from examining the frequency dependence of the $\sigma_2(\omega, 10K) \times \omega$. Advantages and deficiencies of these methods are analyzed in Section II. The latter approach may underestimate the magnitude of λ_c because of the screening effects associated with the response of unpaired charge carriers at $T \ll T_c$. We employed a Kramers-Kronig transformation (Eqs. 3 and 4) to correct for this effect (solid line in panel D).

FIG. 2. The c -axis penetration depth $\lambda_c(T = 0K)$ as a function of the c -axis DC conductivity $\sigma_{DC}(T_c)$. We find two distinct patterns of $\lambda_c - \sigma_{DC}$ scaling. Cuprate superconductors exhibit much shorter penetration depths than non-cuprates materials with the same $\sigma_{DC}(T_c)$. This result implies a dramatic enhancement of the energy scale Ω_C from which the condensate is collected as described in the text. The superconducting transition temperature T_c has not been found to be relevant to the $\lambda_c - \sigma_{DC}$ scaling. Data points: YBCO (Ref. 6,15,17), overdoped YBCO (Ref. 12–15), La214 (Ref. 6,16,18,33), HgBa₂Cu₂O₄ (Ref. 34,59), Tl2201 (Ref. 2,10,35), Bi₂Sr₂CaCu₂O₈ (Ref. 7,23), Nd_{2-x}Ce_xCuO₄ (Ref. 8,27). Blue points - underdoped (UD), green - optimally doped (OpD); red - overdoped (OD). Transition metal dichalcogenides (Ref. 19–21,47,60–62), (ET)₂X compounds (Ref. 22,24,25,28–30,63–65), (TMTSF)₂ClO₄ (Ref. 66,67), Sr₂RuO₄ (Ref. 26,68), niobium (Ref. 31,32), lead (Ref. 32), niobium Josephson junctions (Ref. 69) and α Mo_{1-x}Ge_x (Ref. 70). Inset: in a conventional dirty limit superconductor the spectral weight of the superconducting condensate (given by $1/\lambda^2$) is collected primarily from the energy gap region. The total normal weight is preset by magnitude of σ_{DC} whereas the product of $2\Delta \times \sigma_{DC}$ quantifies the fraction of the weight that condenses.

FIG. 3. Examples of the interplane transport for layered superconductors. Top panels show the out-of-plane optical conductivity $\sigma_c(\omega)$, the bottom panels the corresponding in-plane scattering rate $1/\tau_{ab}(\omega)$. The observation of the Drude-like feature in the interplane optical conductivity of the dichalcogenide 2H-NbSe₂ (top-right panel) is consistent with magnetoresistance measurements that revealed evidence for well-behaved quasiparticles. In contrast the conductivity of underdoped YBa₂Cu₃O_{6.6} material (top-left panel) gives no signs of coherent response. Overdoped cuprates show the emergence of a Drude-like feature (top-middle panel) and also occupy an intermediate position between the two lines in Fig. 2. Experimental data: YBa₂Cu₃O_{6.6} (Ref. 52,71), YBa₂Cu₃O₇ (Ref. 13,14), YBa₂Cu₃O_{6.95} (Ref. 52) and 2H-NbSe₂ (Ref. 46).

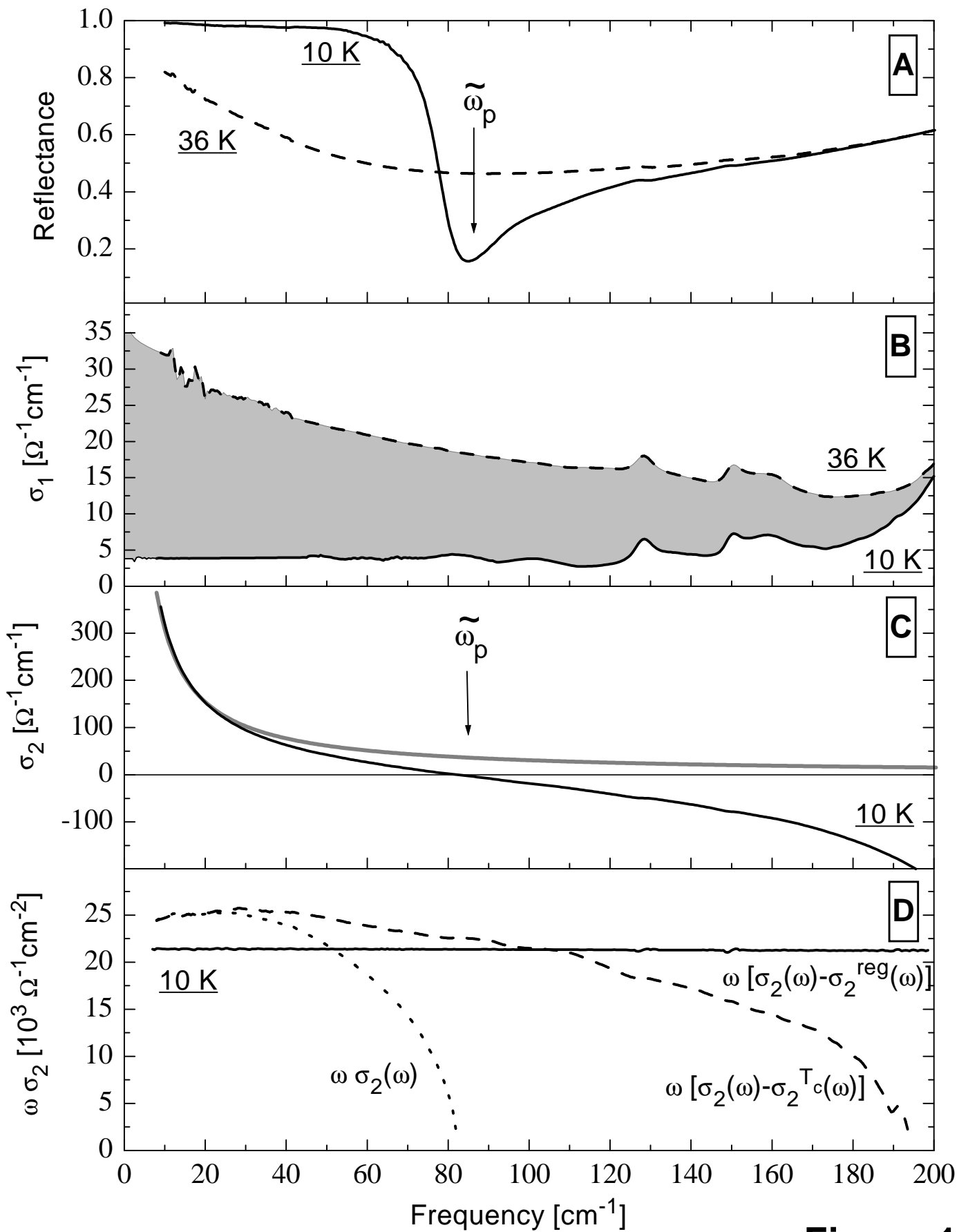


Figure 1

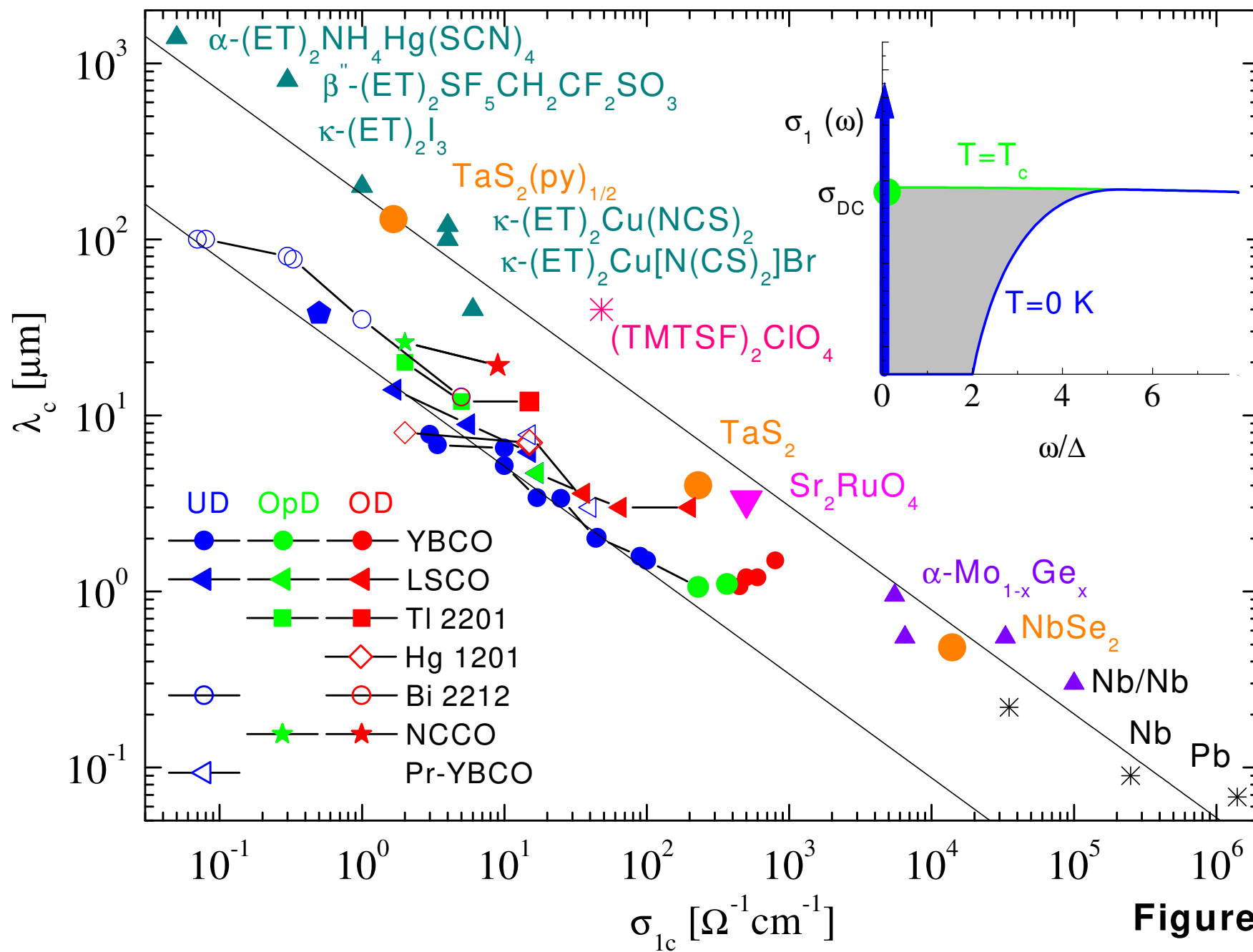


Figure 2

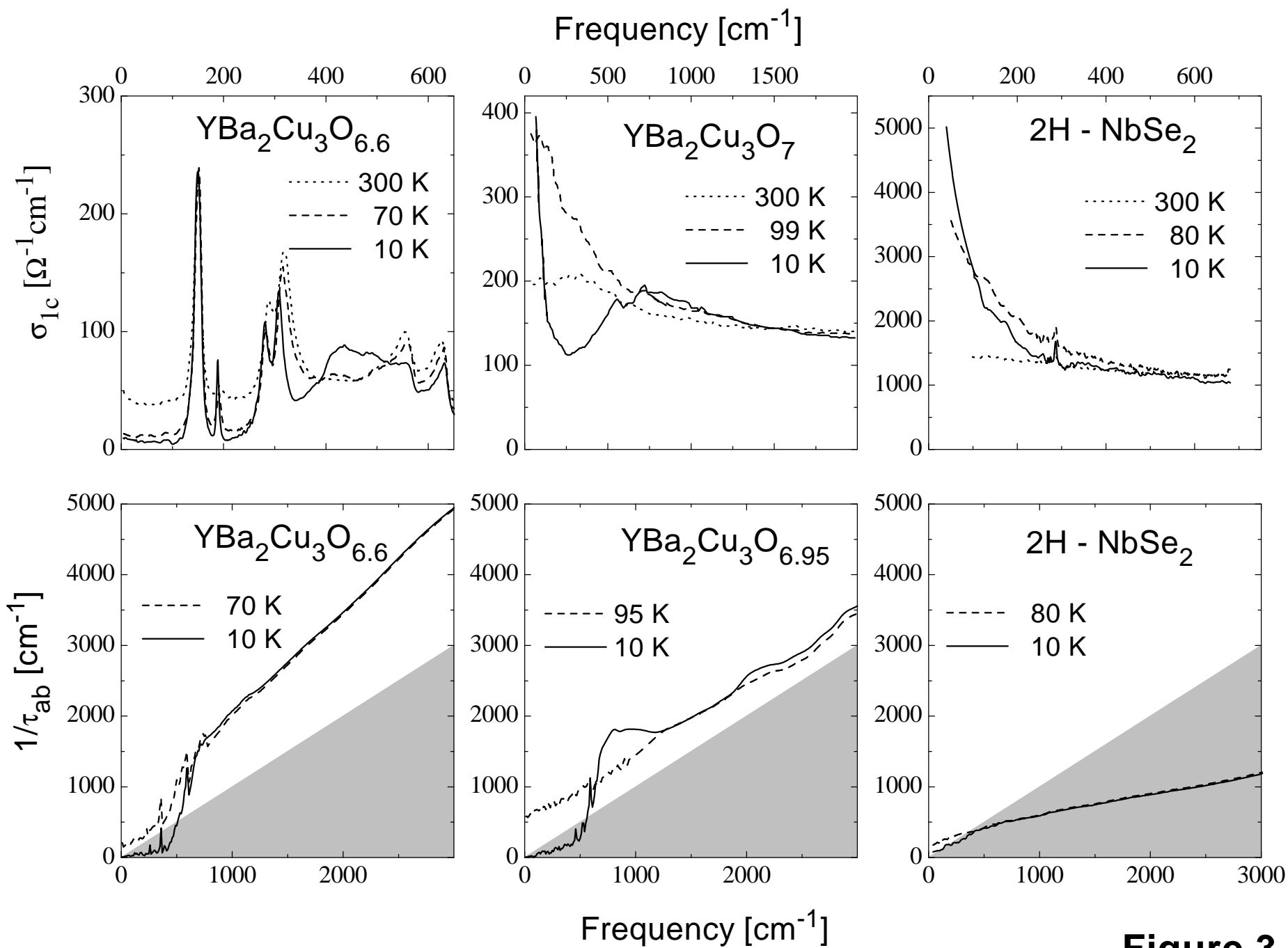


Figure 3